ELSEVIER

Chemical Engineering Journal 129 (2007) 153–159

Chemical Engineering Journal

www.elsevier.com/locate/cej

Photocatalytic decolorization of anthraquinonic dye by TiO_2 thin film under UVA and visible-light irradiation

C.H. Ao [a], M.K.H. Leung [a,*], Ringo C.W. Lam [a], Dennis Y.C. Leung [a], Lilian L.P. Vrijmoed [b], W.C. Yam [c], S.P. Ng [c]

[a] *Department of Mechanical Engineering, The University of Hong Kong, Pokfulam Road, Hong Kong, China*
[b] *Department of Biology and Chemistry, City University of Hong Kong, Hong Kong, China*
[c] *Department of Microbiology, The University of Hong Kong, Hong Kong, China*

Received 28 March 2006; received in revised form 10 October 2006; accepted 23 October 2006

Abstract

In this investigation, the effectiveness of using photocatalytic sol–gel TiO_2 thin film to decolorize anthraquinonic dye Acid Blue 80 was evaluated experimentally. The TiO_2 photocatalysts synthesized were characterized by DSC–TG, XRD, HRTEM, UV–vis spectra, SEM, and XPS. The experimental results showed that a TiO_2 thin film formed without high temperature calcination could effectively perform photocatalytic decolorization under UVA irradiation. After the TiO_2 thin film was modified by Cr ion implantation, the characterization by UV–vis spectra showed that the light absorption was extended beyond UV to the visible range. The modified thin film could perform visible-light-assisted photocatalytic decolorization of the dye. The overall study demonstrates the promise of solar photocatalytic decolorization of dye for treatment of textile effluent. By adopting immobilized TiO_2 thin films instead of conventional suspended TiO_2 particles, the photocatalytic water treatment method becomes more cost-effective as the costly filtration process, normally needed to recover TiO_2 particles from the effluent discharge, can be omitted.

Keywords: Photocatalytic decolorization; Titanium dioxide; Sol–gel thin film; Anthraquinonic dye; Chromium ion implantation

1. Introduction

The textile industry is expanding worldwide especially in the developing countries. In response to the continuous increase in effluent discharge from textile factories, it is necessary to develop effective and low-cost wastewater treatment methods. Existing methods, such as reverse osmosis, ultra-filtration, and adsorption, are efficient mitigation measures but the costs are high.

Advanced oxidation processes, particularly photocatalytic oxidation technology, offer promising wastewater treatment alternatives. Titanium dioxide (TiO_2), a viable photocatalyst, capable of oxidizing various pollutants, is non-toxic, chemically stable, inexpensive, and commercially available [1–4]. Relevant studies showed that TiO_2 photocatalysis could perform decolorization of different dyes, such as Acid Blue 80 [5], Acid Orange 52 [6], Reactive Red 239 [7], Procion Red MX-5B [8], and Solopheny Green [9]. The commonality in these studies was the use of TiO_2 suspension in their photocatalytic decolorization systems. In commercial applications, costly separation procedures were required to recover the TiO_2 powder from the treated effluent prior to discharge. Another concern for using TiO_2 suspension was that excessive TiO_2 loading would diminish the light penetration resulting in poor photocatalytic activity [10]. Alternatively, Kim and Park studied photocatalytic decolorization of a dye, rhodamine B, by immobilized TiO_2 on silicone sealant [11].

The aim of the present study was to investigate the photocatalytic decolorization of Acid Blue 80 (molecular structure shown in Fig. 1) by sol–gel TiO_2 thin film and thin film modified by chromium (Cr) ion implantation. When TiO_2 is bombarded with Cr ions accelerated in a high-voltage field, the high-energy ions are injected into the TiO_2 lattice. This process modifies the TiO_2 electronic structure and extends its photo-response to the visible range up to 700 nm [12–18]. The substrate was made of light-transmitting glass material. The photocatalysts synthesized were fully characterized for the chemical contents and crystal structures. Dye decolorization tests using both UVA and visible-light

* Corresponding author. Fax: +852 2858 5415.
E-mail address: mkhleung@hku.hk (M.K.H. Leung).

1385-8947/$ – see front matter © 2006 Elsevier B.V. All rights reserved.
doi:10.1016/j.cej.2006.10.022

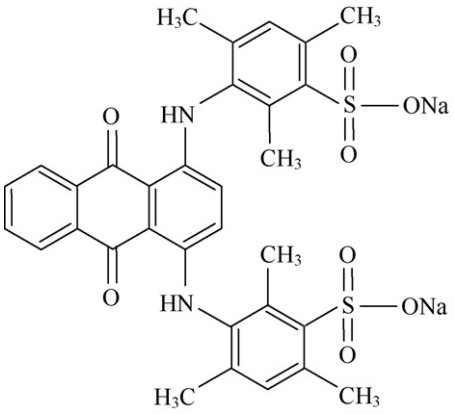

Fig. 1. Molecular structure of Acid Blue 80.

irradiation were conducted. The detailed methodology, experimental results, and reaction kinetics are presented and discussed in this paper.

2. Methodology

2.1. Preparation of TiO_2 thin films and Cr ion implantation

The details of the fabrication of the sol–gel TiO_2 thin films have been described elsewhere [19,20]. The first step was adding 15-ml titanium isopropoxide and 1-ml nitric acid into 150-ml deionized water. The solution was refluxed in a stirring flask at 80 °C for 3 days to produce a sol–gel solution. The sol–gel solution was then evenly applied onto the inner surface of a clean 90-mm borosilicate Petri dish. The TiO_2 coated dish was then heated in an oven at 75 °C for 24 h to drive out all the liquid content to complete the synthesis of the first photocatalytic thin film sample. The weight gain by the thin film was about 7 mg. The second thin film sample was synthesized by the same procedures described above with an additional calcination process at 400 °C for 2 h. The third sample was a visible-light-assisted photocatalytic thin film produced by modification of a TiO_2 thin film of the first sample type by Cr ion implantation (denoted by Cr/TiO_2). In this process, a borosilicate Petri dish coated with a sol–gel TiO_2 thin film was placed inside an ion implanter and the system was evacuated to 1×10^{-7} Torr. Chromium ion beam was produced from a Metal Vapor Vacuum Arc (MEVVA) ion source. The ion implanter was regulated to achieve a loading of 1×10^{17} ion cm^{-2}. The fundamentals and detailed processes of ion implantation can be found in the literature [13,14].

2.2. Catalyst characterization

A Bruker D8 Advance diffractometer employing Cu Kα was used to identify the X-ray diffraction (XRD) pattern and the TiO_2 crystal structure. An accelerating voltage of 40 kV and a current of 40 mA with a scan rate of 0.05° s^{-1} were used. Differential scanning calorimetry (DSC) and thermal gravimetric (TG) analyses were performed together using a NETZSCH STA 449C instrument. A 10-mg photocatalyst removed from a thin film sample by a spatula was tested with a heating rate of 10 °C min^{-1} in flowing air.

The surface morphology of a TiO_2 thin film was obtained by a LEO 1530 field emission scanning electron microscope (SEM). The diffuse reflectance UV–vis absorption spectra of a thin film was obtained by a Perkin-Elmer Lambda 900 UV–vis–NIR spectrophotometer. The compound $BaSO_4$ was used as a reflectance standard in the UV–vis diffuse reflectance experiment. X-ray photoelectron spectroscopy (XPS) tests were conducted by a Physical Electronics 5600 multi-technique system. The surface probe detected electrons generated in a depth within few nanometers on the sample surface. The C 1s peak at 248.8 eV of the surface adventitious carbon was used as a reference for all the binding energy measurements. High resolution transmission electron microscopy (HRTEM) was performed by a Philips Tecnai 200-kV transmission electron microscope.

2.3. Experiments

Experiments were conducted to evaluate the performance of different photocatalytic thin film samples in decolorization of Acid Blue 80. At the beginning of each test, 10-ml diluted Acid Blue 80 (10 ppm and pH 5.78) was dispensed into a photocatalyst-coated Petri dish. The setup was kept in the dark to allow the adsorption of dye to reach a state of equilibrium as a standard starting point of photocatalytic test. During this period, the dye solution was sampled every 10 min. It was found that it took about 30 min for the adsorption to reach the equilibrium state. Then, an 8-W UVA lamp (Philips) placed 50 mm above the Petri dish was turned on. The UVA irradiance was 3 mW cm^{-2} measured by a Lutron UVA 365 light meter. Samples of the dye solution were taken at designated time intervals and analyzed by a calibrated UV–vis spectrophotometer (Spectronic Instrument, Spectronic Genesys 2). The tests were repeated for photocatalyst-coated Petri dish without UVA irradiance and plain Petri dish with UVA irradiance for experimental control.

For testing the visible-light-assisted photocatalytic effect of a Cr/TiO_2 thin film, a 250-W metal halide lamp (Philips) instead of the UVA lamp was placed 400 mm above the Petri dish to produce a visible-light irradiance of 3 mW cm^{-2}. A UV filter was used to block the radiation under 470 nm to ensure that the test was carried out entirely under visible-light irradiation. The experimental procedures followed the same above-mentioned steps. For testing each combination of material and operational parameters, dye absorbance measurements were taken to obtain the maximum, minimum and mean values of the dye concentration at different time intervals.

3. Results and discussion

3.1. Characteristics of photocatalysts

Fig. 2 presents the results of the DSC–TG analysis of the sol–gel TiO_2 photocatalyst finished by a drying process at 75 °C. Two stages of weight loss were observed from the TG curve: (1) 11% weight loss from room temperature to 375 °C and (2) 6% weight loss from 375 to 975 °C. The first stage of weight loss

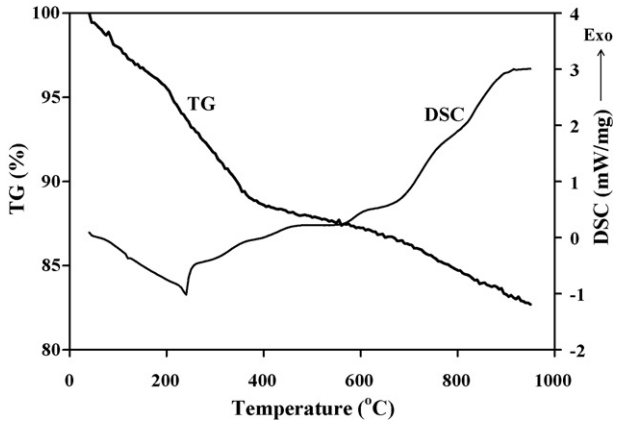

Fig. 2. DSC–TG analysis of photocatalyst TiO_2.

referred to the evaporation of physically adsorbed water. The second stage of weight loss was due to the chemisorbed water and residual organics in the photocatalyst [21]. From the DSC curve, an endothermic peak was found at 240 °C, the boiling point of titanium isopropoxide used as the parent chemical solution. The endothermic peak was due to the energy required for vaporization of the titanium isopropoxide. No exothermic peak was observed as the sample was heated up to 900 °C. The results implied the absence of crystallization [21,22].

As shown in Fig. 3, the XRD diffraction patterns of both TiO_2 photocatalyst dried at 75 °C and TiO_2 calcined at 400 °C showed anatase peaks at 25.4° with reference to the 21–1272 anatase ASTM card. Formation of brookite phase was also observed at 30.8 °C in both TiO_2 samples. The XRD results, consistent with the previous DSC–TG results, indicated no new crystal phase formation in the calcination process. The sol–gel thin film was crystallized when it was dried at 75 °C. The crystallinity of the TiO_2 calcined at 400 °C was higher because a higher thermal energy was applied in the synthesis process [23].

Scherrer's equation is widely used to determine the crystallite size of the TiO_2 particles from the (1 0 1) plane diffraction peak [24,25]. The calculated crystal sizes of TiO_2 dried at 75 °C and TiO_2 calcined at 400 °C were found to be 3.2 and 7.5 nm, respectively. The SEM images of the calcined sample shown in

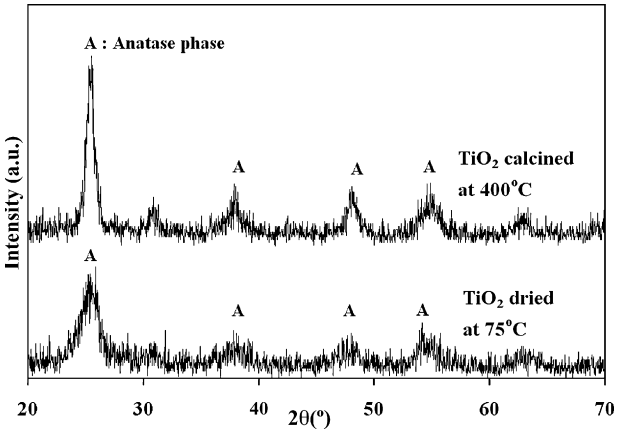

Fig. 3. XRD pattern of TiO_2 photocatalyst.

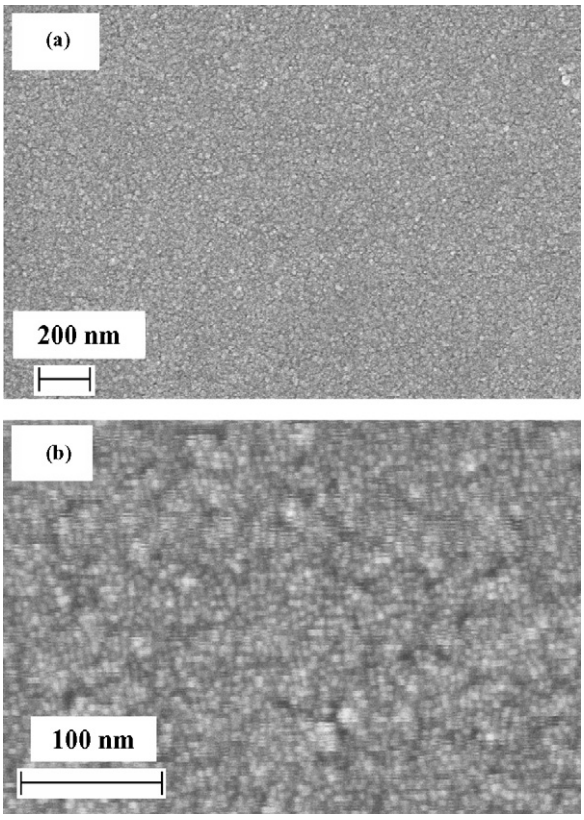

Fig. 4. SEM micrographs of TiO_2 calcined at 400 °C.

Fig. 4 display the TiO_2 spherical particles. HTREM analyses were also performed to obtain the crystal phase and crystal size of TiO_2. As shown in Fig. 5, the measured crystal size of the TiO_2 dried at 75 °C was about 7.4 nm (measured by Gatan), in a

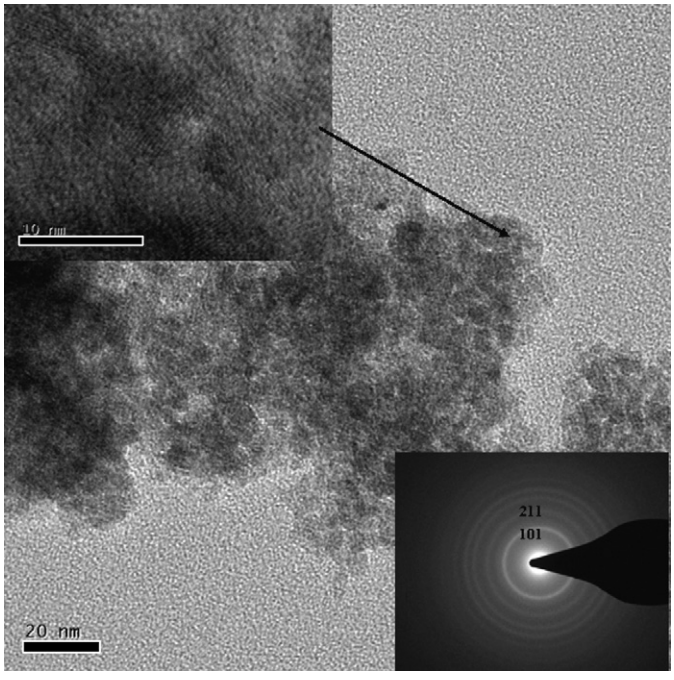

Fig. 5. HRETM of TiO_2 dried at 75 °C (left insert: electron diffraction pattern of TiO_2; right insert: lattice fringe of TiO_2).

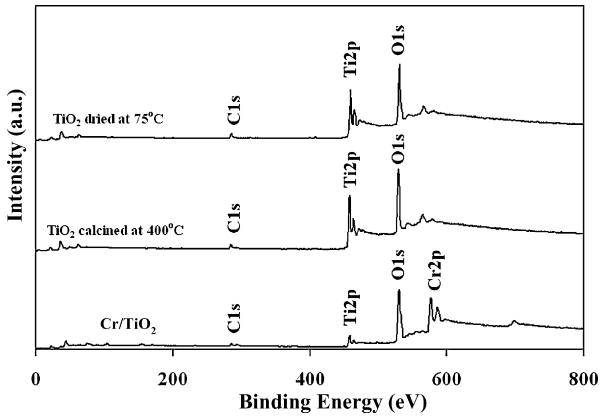

Fig. 6. XPS spectra of TiO_2 and Cr/TiO_2 thin film.

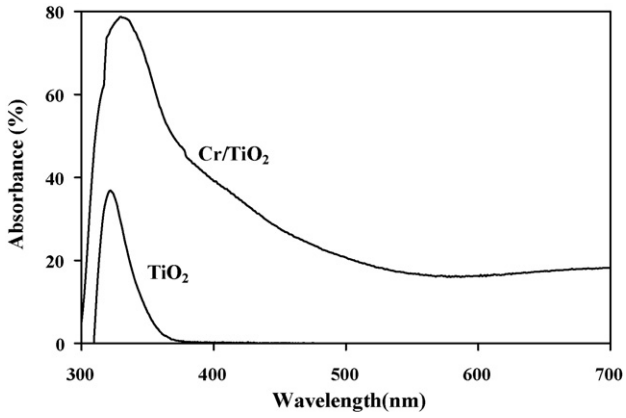

Fig. 7. Diffuse reflectance spectra of TiO_2 and Cr/TiO_2 thin film.

reasonable agreement with the calculated value from the XRD diffraction pattern. The electron diffraction pattern is shown in the right inserted figure. The first ring was assigned as anatase phase (1 0 1) and the second ring was assigned as brookite phase (2 1 1). The findings indicated the presence of the brookite phase. The left inserted figure shows the lattice fringe of the TiO_2 with a spacing of 0.17 nm.

Fig. 6 shows the XPS spectra of the TiO_2 and Cr/TiO_2 thin films. The C 1s peak at 248.8 eV was the adventitious hydrocarbon originated from the analytical instrument. Photoelectron peaks observed at binding energies (E_b) of 458 and 531 eV were corresponding to Ti 2p and O 1s, respectively, for all the TiO_2 thin films with a chemical state of Ti^{4+}. The aforementioned binding energies were the characteristic parameters of TiO_2 [26]. The two distinct peaks observed at E_b equal to 576.8 and 586.4 for the TiO_2 thin film implanted with Cr ion represented the Cr 2p of Cr^{3+} state [27,28]. A study [29] showed that Cr^{4+} might be formed at a binding energy of 597.4 eV. As no peak at 597.4 eV was observed in Fig. 6, the measurements implied the presence of Cr^{3+} state only.

It is reported that chromium ion causes certain toxic effects, such as cellular necrosis by chronic oral exposure [30]. The reported toxic effect, however, is related to Cr^{6+}. At the present moment, Cr^{6+} is as a known a human carcinogen but not Cr^{3+}. The use of Cr^{3+} for wastewater treatment is a feasible approach.

The compositions of the TiO_2 and Cr/TiO_2 thin films are presented in Table 1. The red shift from the UV–vis spectrophotometry analysis, as shown in Fig. 7, also manifests the presence of Cr/TiO_2 in the thin film. The XPS peak of Cr 2p being higher than that of Ti 2p, as shown in Fig. 6, implies deposition of Cr ion on the thin film surface [27,28].

Similar finding of the abovementioned brookite TiO_2 phase was also reported in other studies [31–34]. These studies explained that sodium oxide migrated from the glass substrate into the TiO_2 film during the heat treatment process inhibited the anatase formation and produced the brookite phase. However, different phenomena were observed in the present study. First, no sodium peak was found in the XPS analyses. Second, the XRD pattern and the HRTEM electron diffraction pattern showed the presence of brookite phase even in the TiO_2 photocatalyst dried at 75 °C. Migration of sodium ion is only possible under calcination at a high temperature of several hundred degree Celsius [34]. It was therefore concluded that the brookite phase was formed without the presence of the sodium ion.

Table 1
Composition (at.%) of TiO_2 and Cr/TiO_2 thin film

Thin film	Element (%)		
	Ti	O	Cr
TiO_2 dried at 75 °C	25.7	61.49	0
Cr/TiO_2	4.9	58.66	21.5

Anatase TiO_2 mostly absorbs light with a wavelength shorter than 380 nm [35]. In order to increase the light absorption range, the electronic property of the TiO_2 was modified by Cr ion implantation [13,14,36]. The UV–vis absorption spectra distributions of TiO_2 and Cr/TiO_2 thin films were measured. As shown in Fig. 7, when the TiO_2 thin film was implanted with Cr ion, the absorption of the light spectra was extended to the visible region.

From another study of TiO_2 thin film, interference fringes were observed on a TiO_2 film prepared by a radio-frequency magnetron (RF-MS) deposition method with a high transparency [12]. In this study, no interference fringe was observed (Fig. 7) because the TiO_2 thin film sample exhibited semi-transparency and high absorption in the visible-light spectrum, resulting from non-uniformity of the TiO_2 film prepared by the sol–gel method.

3.2. Decolorization of Acid Blue 80 by UVA irradiation

The UV–vis spectrophotometer was calibrated for measuring the concentration of Acid Blue 80. As shown in Fig. 8, the entire absorption spectrum of Acid Blue 80 was obtained. The peak at 626 nm of the 20-ppm curve was used as the reference [37]. The test results of the decolorization of Acid Blue 80 by the two TiO_2 reactors under UVA irradiation are shown in Fig. 9. The absence of either TiO_2 or UVA irradiation, served as control experiments, caused no decolorization effect. These results also implied negligible photolysis and adsorption effects [38]. For the presence of both TiO_2 and UVA irradiation, the decolorization rate was significant and complete decolorization was obtained after 360 min.

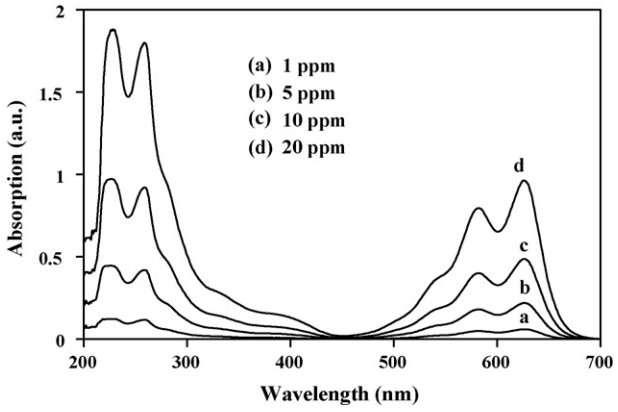

Fig. 8. Absorption spectra of Acid Blue 80.

In general, the dye decolorization behavior closely follows the Langmuir–Hinshelwood (L-H) kinetics model [1,6,39]:

$$r = -\frac{dC}{dt} = \frac{kKC}{1 + KC} \quad (1)$$

where C is the Acid Blue 80 concentration (ppm) at time t (min), k the reaction rate constant (ppm min^{-1}), and K is the adsorption coefficient of Acid Blue 80 (ppm^{-1}). The integration of Eq. (1) is:

$$t = \frac{1}{Kk} \ln\left(\frac{C_0}{C}\right) + \frac{1}{k}(C_0 - C) \quad (2)$$

As the initial concentration is in the order of ppm, the second term on the right-hand side of Eq. (2) is relatively negligible. Therefore, Eq. (2) can be further simplified to [1,6,40]:

$$\ln\left(\frac{C_0}{C}\right) \cong kKt = k't \quad (3)$$

where k' is the apparent rate constant (min^{-1}).

For the experimental measurements presented in Fig. 9, it was found that the apparent rate constant k' of the TiO_2 thin film dried at 75 °C was 0.01125 min^{-1} and k' of the one with additional calcination at 400 °C was 0.01132 min^{-1}, a slightly higher value. These results did not agree with the findings in other studies [34,41–43] showing that the amount of sodium migration from the glass substrate to the TiO_2 thin film increased with the calcination temperature resulting in a lower photocatalytic activity. As the TiO_2 thin film dried at 75 °C already possessed photocatalytic reactivity, material of low-melting point, such as polymer, could be selected as the substrate material.

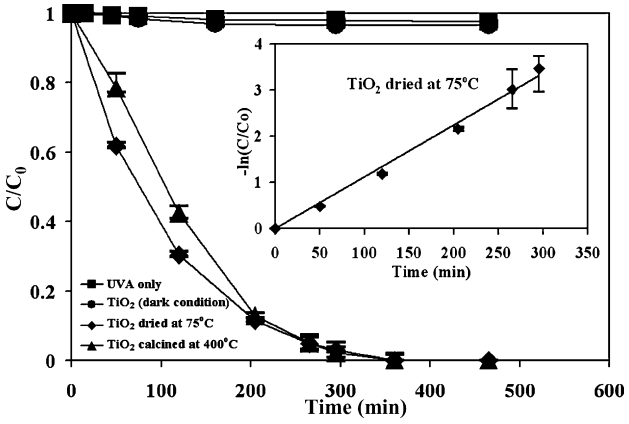

Fig. 9. Decolorization of Acid Blue 80 by TiO_2 under UVA irradiation.

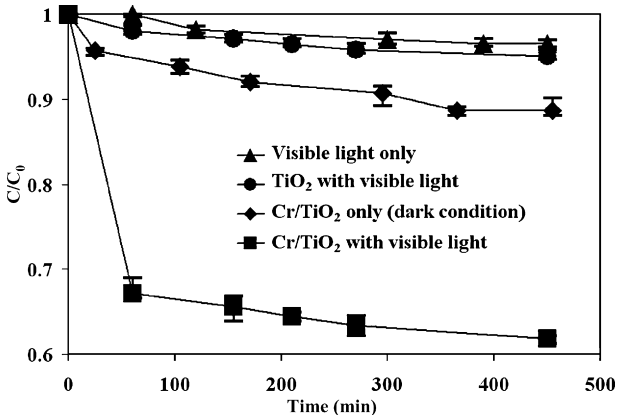

Fig. 10. Decolorization of Acid Blue 80 by Cr/TiO_2 under visible-light irradiation.

3.3. Decolorization of Acid Blue 80 by visible-light irradiation

Fig. 10 presents the visible-light irradiation test results. The four tests with different combinations of photocatalyst and irradiation clearly exhibited the effectiveness of Cr/TiO_2 irradiated by visible-light for decolorization of Acid Blue 80. The photocatalytic oxidation reaction was activated due to the extension of absorption spectra to visible-light by Cr ion implantation. The reaction rate decreased with irradiance time after 60 min because a competition for photodegradation might occur between the reactant and the intermediate product. The slow down of the dye degradation might be also due to heavy adsorption of intermediate products that could not be degraded by visible-light photocatalysis [1].

In other related dye decolorization studies [6,44], TiO_2 without any modification under visible-light irradiation could decolorize aminoazobenzene Acid Orange 52 and eosin. The chemical reactions involved excitation of adsorbed TiO_2 to the singlet or triplet state and electron injection from the excited dye to the conduction band of TiO_2. As a result of photosensitized oxidation, the dye molecules were converted into the cationic dye radicals [1,44]. However, in this study, the TiO_2 thin film without the presence of Cr ion failed to perform any decolorization effect under visible-light irradiation. It implied that there was no photosensitized oxidation effect.

4. Conclusion

The performance of photocatalytic decolorization of anthraquinonic dye Acid Blue 80 was tested experimentally. The parametric experimental results showed that there was no photosensitized oxidation effect and the visible-light-assisted photocatalysis was entirely due to the extension of activating

spectrum to the visible range by the implanted Cr ion. Both TiO_2 under UVA irradiation and Cr/TiO_2 under visible-light irradiation were found effective in decolorization of dye. Hence, the investigation has demonstrated the promise of using solar energy, which consists of much UV and visible-light, to activate photocatalysis to clean textile effluent discharge. In the preparation of TiO_2 photocatalyst, the crystal structures of anatase and brookite were formed on the sol–gel TiO_2 thin film after the low-temperature drying process at 75 °C. It implies that materials of low melting points, such as polymers, can be effectively used as substrate materials for the sol–gel coating method.

Acknowledgements

The study was supported by a grant from the Innovation and Technology Commission (ITS/076/03) and a grant from the Research Grants Council (HKU 7150/05E) of the Hong Kong Special Administrative Region, China.

References

[1] I.K. Konstantinou, T.A. Albanis, TiO_2-assisted photocatalytic degradation of azo dyes in aqueous solution: kinetic and mechanistic investigations: a review, Appl. Catal. B 49 (2004) 1–14.

[2] C.H. Ao, S.C. Lee, C.L. Mak, L.Y. Chan, Photodegradation of volatile organic compounds (VOCs) and NO for indoor air purification using TiO_2: promotion versus inhibition effect of NO, Appl. Catal. B 42 (2003) 119–129.

[3] C.H. Ao, S.C. Lee, J.Z. Yu, J.H. Yu, Photodegradation of formaldehyde by photocatalyst TiO_2: effects on the presences of NO, SO_2 and VOCs, Appl. Catal. B 54 (2004) 41–50.

[4] J.C. Yu, J.G. Yu, J.C. Zhao, Enhanced photocatalytic activity of mesoporous and ordinary TiO_2 thin films by sulfuric acid treatment, Appl. Catal. B 36 (2002) 31–43.

[5] A.B. Prevot, C. Baiocchi, M.C. Brussino, E. Pramauro, P. Savarino, V. Augugliaro, G. Marc, L. Palmisano, Photocatalytic degradation of Acid Blue 80 in aqueous solutions containing TiO_2 suspensions, Environ. Sci. Technol. 35 (2001) 971–976.

[6] C. Galindo, P. Jacques, A. Kalt, Photodegradation of the aminoazobenzene acid orange 52 by three advanced oxidation processes: UV/H_2O_2, UV/TiO_2 and vis/TiO_2. Comparative mechanistic and kinetic investigations, J. Photochem. Photobiol. A 130 (2000) 35–47.

[7] H.L. Liu, Y.R. Chiou, Optimal decolorization efficiency of Reactive Red 239 by UV/TiO_2 photocatalytic process coupled with response surface methodology, Chem. Eng. J. 112 (2005) 173–179.

[8] C. Hu, J.C. Yu, Z. Hao, P.K. Wong, Photocatalytic degradation of triazine-containing azo dyes in aqueous TiO_2 suspensions, Appl. Catal. B 42 (2003) 47–55.

[9] C.G. da Silva, J.L. Faria, Photochemical and photocatalytic degradation of an azo dye in aqueous solution by UV irradiation, J. Photochem. Photobiol. A 155 (2003) 133–143.

[10] B. Neppolian, H.C. Choi, S. Sakthivel, B. Arabindoo, V. Murugesan, Solar light induced and TiO_2 assisted degradation of textile dye Reactive Blue 4, Chemosphere 46 (2002) 1173–1181.

[11] D.S. Kim, Y.S. Park, Photocatalytic decolorization of rhodamine B by immobilized TiO_2 onto silicone sealant, Chem. Eng. J. 116 (2006) 133–137.

[12] M. Anpo, Preparation, characterization, and reactivities of highly functional titanium oxide-based photocatalysts able to operate under UV–visible light irradiation: approaches in realizing high efficiency in the use of visible light, Bull. Chem. Soc. Jpn. 77 (2004) 1427–1442.

[13] H. Yamashita, M. Anpo, Application of an ion beam technique for the design of visible light-sensitive, highly efficient and highly selective photocatalyst: ion-implantation and ionized cluster beam methods, Catal. Surv. Asia 8 (2004) 35–45.

[14] M. Anpo, M. Takeuchi, The design and development of highly reactive titanium oxide photocatalysts operating under visible light irradiation, J. Catal. 216 (2003) 505–516.

[15] H. Yamashita, M. Harada, J. Misaka, M. Takeuchi, K. Ikeue, M. Anpo, Degradation of propanol diluted in water under visible light irradiation using metal ion-implanted titanium dioxide photocatalysts, J. Photochem. Photobiol. A 148 (2002) 257–261.

[16] M. Anpo, S. Kishiguchi, Y. Ichihashi, M. Takeuchi, H. Yamashita, K. Ikeue, B. Morin, A. Davidson, M. Che, The design and development of second-generation titanium oxide photocatalysts able to operate under visible light irradiation by applying a metal-ion implantation method, Res. Chem. Intermed. 27 (2001) 459–467.

[17] M. Takeuchi, H. Yamashita, M. Matsuoka, M. Anpo, T. Hirao, N. Itoh, N. Iwamoto, Photocatalytic decomposition of NO under visible light irradiation on the Cr-ion-implanted TiO_2 thin film photocatalyst, Catal. Lett. 67 (2000) 135–137.

[18] S. Nakao, T. Nonami, P. Jin, Y. Miyagawa, S. Miyagawa, High-energy metal ion implantation into titanium dioxide films, Surf. Coat. Technol. 128/129 (2000) 446–449.

[19] W.H. Ching, M. Leung, D.Y.C. Leung, Solar photocatalytic degradation of gaseous formaldehyde by sol–gel TiO_2 thin film for enhancement of indoor air quality, Sol. Energy 77 (2004) 129–135.

[20] M.H.K. Leung, S.M. Tang, R.C.W. Lam, Y.C.L. Leung, W.C. Yam, S.P. Ng, L.L.P. Vrijmoed, Parallel-plate solar photocatalytic reactor for air purification: semi-empirical correlation, modeling, and optimization, Sol. Energy 80 (2006) 949–955.

[21] I.A. Montoya, T. Viveros, J.M. Dominguez, L.A. Canales, I. Schifter, On the effects of the sol–gel synthesis parameters on textural and structural characteristics of TiO_2, Catal. Lett. 15 (1992) 207–217.

[22] K.C. Song, S.E. Pratsinis, The effect of alcohol solvents on the porosity and phase composition of titania, J. Colloid Interf. Sci. 231 (2000) 289–298.

[23] Y.F. Chen, C.Y. Lee, M.Y. Yeng, H.T. Chiu, The effect of calcination temperature on the crystallinity of TiO_2 nanopowders, J. Cryst. Growth 247 (2003) 363–370.

[24] J. Lin, J.C. Yu, An investigation on photocatalytic activities of mixed TiO_2-rare earth oxides for the oxidation of acetone in air, J. Photochem. Photobiol. A 116 (1998) 63–67.

[25] X. You, F. Chen, J. Zhang, Effects of calcination on the physical and photocatalytic properties of TiO_2 powders prepared by sol–gel template method, J. Sol–Gel Sci. Technol. 34 (2005) 181–187.

[26] A. Fernandez, A. Caballero, A.R. Gonzalezelipe, Size and support effects in the photoelectron-spectra of small TiO_2 particles, Surf. Interf. Anal. 18 (1992) 392–396.

[27] Y.X. Li, W. Wlodarski, K. Galatsis, S.H. Moslih, J. Cole, S. Russo, N. Rockelmann, Gas sensing properties of p-type semiconducting Cr-doped TiO_2 thin films, Sens. Actuators B: Chem. 83 (2002) 160–163.

[28] A.M. Salvi, J.E. Castle, J.F. Watts, E. Desimoni, Peak fitting of the chromium 2p XPS spectrum, Appl. Surf. Sci. 90 (1995) 333–341.

[29] I.S. Nam, S.D. Yim, Characteristics of chromium oxides supported on TiO_2 and Al_2O_3 for the decomposition of perchloroethylene, J. Catal. 221 (2004) 601–611.

[30] USPEA, Integrated Risk Information System. Toxicological Review of Trivalent Chromium, USPEA, Washington, DC, 1998.

[31] A. Fernandez, G. Lassaletta, V.M. Jimenez, A. Justo, A.R. Gonzalez-Elipe, J.M. Herrmann, H. Tahiri, Y. Ait-Ichou, Preparation and characterization of TiO_2 photocatalysts supported on various rigid supports (glass, quartz and stainless steel). Comparative studies of photocatalytic activity in water purification, Appl. Catal. B: Environ. 7 (1995) 49–63.

[32] H.G. Yu, J.G. Yu, B. Cheng, C.H. Ao, S.C. Lee, Effects of substrates on the composition and microstructure of TiO_2 thin films prepared by the LPD method, Key Eng. Mater. 280 (2005) 795–800.

[33] T. Watanabe, S. Fukayama, M. Miyauchi, A. Fujishima, K. Hashimoto, Photocatalytic activity and photo-induced wettability conversion of TiO_2 thin film prepared by sol–gel process on a soda-lime glass, J. Sol–Gel Sci. Technol. 19 (2000) 71–76.

[34] Y. Paz, A. Heller, Photo-oxidatively self-cleaning transparent titanium dioxide films on soda lime glass: the deleterious effect of sodium contamination and its prevention, J. Mater. Res. 12 (1997) 2759–2766.

[35] J.L. Gole, J.D. Stout, C. Burda, Y. Lou, X. Chen, Highly efficiency formation of visible light tunable $TiO_{2-x}N_x$ photocatalyst and their transformation at the nanoscale, J. Phys. Chem. B 108 (2004) 1230–1240.
[36] K.K.H. Choy, J.F. Porter, G. Mckay, Intraparticle diffusion in single and multicomponent acid dye adsorption from wastewater onto carbon, Chem. Eng. J. 103 (2004) 133–145.
[37] A.Y. Sychev, Z.O. Anikina, T.V. Isaak, N.I. Tsyntsaru, Formal bleaching kinetics of Acid Blue 80 in weakly acidic, neutral, and basic aqueous media, Russ. J. Gen. Chem. 74 (2004) 376–378.
[38] A.K. Gupta, A. Pal, C. Sahoo, Photocatalytic degradation of a mixture of Crystal Violet (Basic Violet 3) and Methyl Red dye in aqueous suspensions using Ag^+ doped TiO_2, Dye Pigments 69 (2006) 224–232.
[39] Y.M. Xu, C.H. Langford, UV- or visible-light-induced degradation of X3B on TiO_2 nanoparticles: the influence of adsorption, Langmuir 17 (2001) 897–902.
[40] W.Z. Tang, H. An, UV/TiO_2 photocatalytic oxidation of commercial dyes in aqueous-solutions, Chemosphere 31 (1995) 4157–4170.
[41] S.H. Oh, J.S. Kim, J.S. Chung, E.J. Kim, S.H. Hahn, Crystallization and photoactivity of TiO_2 films formed on soda lime glass by a sol–gel dip-coating process, Chem. Eng. Commun. 192 (2005) 327–335.
[42] J.G. Yu, X.J. Zhoa, Q.N. Zhao, Effect of surface structure on photocatalytic activity of TiO_2 thin films prepared by sol–gel method, Thin Solid Films 379 (2000) 7–14.
[43] J.S. Liang, Y.W. Feng, G.C. Liang, Z.J. Ji, J. Wang, X.W. Yan, Z.Z. Jin, Effects of post-treatment on the photocatalytic activity of mesoporous TiO_2 thin films, J. Mater. Sci. Lett. 22 (2003) 1503–1506.
[44] F.L. Zhang, J.C. Zhao, T. Shen, H. Hidaka, E. Pelizzetti, N. Serpone, TiO_2-assisted photodegradation of dye pollutants-II. Adsorption and degradation kinetics of eosin in TiO_2 dispersions under visible light irradiation, Appl. Catal. B: Environ. 15 (1998) 147–156.